Introduction of exogenous wild-type *p53* mediates the regulation of oncoprotein 18/stathmin signaling via nuclear factor-κB in non-small cell lung cancer NCI-H1299 cells

SANGYAN CHEN[1], YAN ZHAO[1], FANG SHEN[1,2], DAN LONG[1], TING YU[1] and XUECHI LIN[1,2]

[1]Department of Medical Laboratory, Changsha Medical University, Changsha, Hunan 410219;
[2]Department of Clinical Laboratory, The First Affiliated Hospital of Hunan Normal University, Changsha, Hunan 410000, P.R. China

Received March 1, 2018; Accepted December 18, 2018

DOI: 10.3892/or.2019.6964

Abstract. Our previous studies demonstrated that high expression of oncoprotein 18 (Op18)/stathmin promotes malignant transformation of non-small cell lung cancer NCI-H1299 cells. Investigation of the cellular settings determined that NCI-H1299 cells were genetically *p53* deficient. In order to determine whether *p53* deficiency is associated with Op18/stathmin-mediated high levels of malignancy, exogenous wild-type *p53* ($p53^{wt}$) was introduced into NCI-H1299 cells in the present study to observe Op18/stathmin signaling changes and malignant behaviors. The results indicated that p53 downregulated Op18/stathmin expression and phosphorylation at the Ser25 and Ser63 sites in NCI-H1299 cells, and the abilities of proliferation, colony formation and migration in multi-dimensional spaces were simultaneously reduced. Introduction of $p53^{wt}$ inhibited the expression of the transcription factor nuclear factor-κB (NF-κB), and the activities of the Op18/stathmin upstream kinases cyclin-dependent 2 (CDC2) and extracellular signal-regulated kinase (ERK). Furthermore, blocking of NF-κB signaling decreased CDC2 and ERK activation. Additionally, p53 intervention attenuated the secretion and protein expression of the immune inhibitory cytokine interleukin-10, which was in accordance with the effect of NF-κB signaling inhibition. Further experiments validated that p53 enhanced the sensitivity of NCI-H1299 cells to Taxol through initiating the caspase-3 and -9 intrinsic death pathways, and resulted in cell cycle arrest at the G_1/S phases. These data indicated that exogenous $p53^{wt}$ mediates the regulation of Op18/stathmin signaling through the p53-NF-κB-CDC2/ERK-Op18/stathmin pathway, and that p53 deficiency is associated with high malignancy levels of NCI-H1299 cells.

Correspondence to: Professor Xuechi Lin, Department of Medical Laboratory, Changsha Medical University, 1501 Leifeng Road, Changsha, Hunan 410219, P.R. China
E-mail: xuechilin71@126.com

Key words: p53, oncoprotein 18/stathmin, nuclear factor-κB, signal regulation, NCI-H1299 cells

Introduction

In our previous study, 5 epithelial-derived carcinoma cell lines, including human non-small cell lung cancer (NSCLC) NCI-H1299, human nasopharyngeal carcinoma CNE1, human gastric cancer MGC, human breast cancer MCF-7 and human hepatoma Hep3b-2, were used to screen Taxol-resistant cells. The results confirmed that NCI-H1299 cells highly expressing oncoprotein 18 (Op18)/stathmin exhibited resistance to Taxol, and strong capabilities of cell proliferation, migration and invasion, compared with the other cell lines (1). Silencing of Op18/stathmin by RNA interference (RNAi) resulted in inhibition of cell proliferation and motility, and strengthened the sensitivity of NCI-H1299 cells to Taxol. *In vivo* experiments confirmed that RNAi of Op18/stathmin combined with Taxol co-operatively decreased the tumorigenesis of transplanted NCI-H1299 cells and tumor growth, and promoted high-grade differentiation of xenografts (2). By tracing the genetic background of NCI-H1299 cells and retrieving relative literatures, it was determined that NCI-H1299 cells are innately p53 deficient, and lack p53 protein expression (3,4). We hypothesized that p53 deficiency is associated with the high malignancy levels of NCI-H1299 cells exhibiting high expression of Op18/stathmin.

Wild-type *p53* ($p53^{wt}$) prevents cell cycle progression and the repair of damaged and mutant genes, and induces apoptosis and inhibition of proliferation in tumor development. $p53^{wt}$ is activated and highly expressed in instances of DNA damage caused by stress, including ultraviolet radiation, hypoxia and drugs, promotes the sensitivity of tumors to treatment and increases cell apoptosis (5,6). The majority of antitumor drugs induce p53 expression and activation; for example, in colon cancer HCT-116 cells with $p53^{wt}$ introduced, Adriamycin enhanced p53 expression and inhibition of cell proliferation (7). Similarly, high concentrations of Nutlin-3 induced high expression of p53 resulting in apoptosis in colon cancer RKO and prostate cancer LNCaP cells with $p53^{wt}$, and the status of cell apoptosis was positively associated with the levels of p53 expression (8).

The microtubule regulator Op18/stathmin, a small molecule of phosphoprotein that is highly expressed in solid tumors, serves a crucial role in integrating and transducing various signals from intra- and extra-cellular stimuli (9). It directly regulates the dynamics equilibrium of the microtubule cytoskeleton, and controls cellular biological behavior, including cell cycle progression, metastasis and invasion, through phosphorylated inactivation and dephosphorylated activation (9-11). Co-transfection of Op18/stathmin luciferase reporter and *p53^{wt}* carrier confirmed that *p53^{wt}* inhibited the promoter of Op18/stathmin, which resulted in decreased Op18/stathmin mRNA transcription and protein expression, and arrested the cell cycle at the G_2/M phases in HT1080 fibrosarcoma cells (12).

The present study is a continuation of our previous research which primarily focused on investigating whether *p53^{wt}* deficiency was associated with Taxol resistance mediated by Op18/stathmin signaling in NCI-H1299 cells. Additionally, the changes in Taxol resistance following the introduction of exogenous *p53^{wt}* and the molecular mechanism regulating Op18/stathmin signaling was investigated to determine the effects of exogenous *p53^{wt}* on Op18/stathmin signaling and the underlying molecular mechanisms, and the association between p53 deficiency and the malignancy of NCI-H1299 cells was confirmed.

Materials and methods

Cell lines and cell culture. The NSCLC NCI-H1299 cell line [American Type Culture Collection (ATCC), Manassas, VA, USA; ATCC number, CRL-5803™] was grown in RPMI-1640 medium (cat. no. 01-100-1ACS; Biological Industries, Kibbutz Beit Haemek, Israel) supplemented with 10% fetal bovine serum (FBS; cat. no. 04-001-1ACS; Biological Industries), 100 IU/ml penicillin and 100 μg/ml streptomycin (cat. no. SV30010; HyCone; GE Healthcare Life Sciences, Logan, UT, USA) at 37˚C in humidified atmosphere containing 5% CO_2.

Antibodies and chemical reagents. The primary antibodies comprised of rabbit polyclonal anti-stathmin (1:3,000; cat. no. 569391; EMD Millipore, Billerica, MA, USA), anti-extracellular signal-regulated kinase 1 (ERK1; 1:1,000; cat. no. sc-93), anti-cyclin-dependent 2 (CDC2; 1:1,000; cat. no. sc-954), anti-nuclear factor-κB (NF-κB; 1:1,000; cat. no. SC-109), anti-B-cell lymphoma-2 (Bcl-2; 1:1,000; cat. no. sc-492), mouse monoclonal anti-β-actin (1:2,000; cat. no. sc-47778), anti-phospho(p)-ERK1 (1:1,000; cat. no. sc-7383), anti-caspase-3 (1:1,000; cat. no. sc-7272), anti-p53 (1:1,000; cat. no. sc-126), anti-Bcl-2-associated X protein (1:1,000; Bax; cat. no. sc-7480) (Santa Cruz Biotechnology, Inc., Dallas, TX, USA), mouse monoclonal anti-caspase-8 (1:1,000; cat. no. 9746), rabbit monoclonal anti-caspase-9 (1:1,000; cat. no. 9502), rabbit polyclonal anti-p-thr161-CDC2 (1:1,000; cat. no. 9114) (Cell Signaling Technology, Inc., Danvers, MA, USA), anti-p-stathmin Ser25 (1:1,000; cat. no. ab194752), anti-p-stathmin Ser63 (1:1,000; cat. no. ab76583), anti-interleukin-10 (IL-10; 1:1,000; cat. no. ab34843) and anti-IL-6 (1:1,000; cat. no. ab6672) (Abcam, Cambridge, MA, USA).

The secondary antibodies used were horseradish peroxidase (HRP)-conjugated goat anti-rabbit IgG (which was diluted at 1:3,000 for the detection of stathmin, NF-κB, IL-6 and IL-10, and at 1:2,500 for detecting caspase-9, Bcl-2, p-stathmin-Ser25, -Ser63, phospho-Thr161-CDC2, CDC2 and ERK; cat. no. sc-2004) and rabbit anti-mouse IgG (which was diluted at 1:3,000 for the detection of β-actin and p53, and at 1:2,500 for analyzing caspases-3, -8, Bcl-2-associated X and phosphor-ERK; cat. no. sc-358914) (Santa Cruz Biotechnology, Inc.).

The NF-κB inhibitor ammonium pyrrolidine dithiocarbamate (PDTC; cat. no. 5108-96-3; Sigma-Aldrich; Merck KGaA, Darmstadt, Germany) (13) and Taxol (cat. no. sc-201439; Santa Cruz Biotechnology, Inc.) were separately dissolved in dimethyl sulfoxide (DMSO), stored at -20˚C and diluted to appropriate concentrations (Taxol, 100 nM; or PDTC, 5 or 10 μM) prior to use.

Plasmid construction and cell transfection. Nearly confluent cells at the logarithmic growth phase were divided into three groups (blank, C3 and p53^{wt}) for transfection as follows: Blank control without any plasmid (blank); empty vector *pEGFP-C3* (C3); and pEGFP-C3-p53 (p53^{wt}). The plasmid pEGFP-C3-p53 was constructed by inserting the *p53^{wt}* gene into the pEGFP-C3 vector between the two cleavage sites of *Xho*I and *Kpn*I, and PEGFP-C3 was labeled with neomycin and kanamycin resistance genes. G418 (400 μg/ml; Sigma-Aldrich; Merck KGaA) was used to screen cells following transfection for 5 h. The PEGFP-C3 and pEGFP-C3-p53 plasmids were provided by Professor Cao Ya (Cancer Research Institute, Central South University, Changsha, China).

Cell transfection was performed with Lipofectamine® 2000 (cat. no. 11668-019; Invitrogen; Thermo Fisher Scientific, Inc.) according to the manufacturer's protocols. Additionally 4 μg plasmids in 10 μl Lipofectamine 2000 were transiently transfected into cells at a transfection efficiency of >80% in 250 μl incomplete RPMI-1640 medium.

Western blot analysis. Protein was extracted with lysis buffer consisting of 50 mM pH 8.0 Tris-HCl, 1 mM ethylenediaminetetraacetic acid, 2% SDS, 5 mM dithiothreitol and 10 mM phenylmethylsulfonyl fluoride. The protein concentration was determined using BCA Protein Assay Reagent (Pierce; Thermo Fisher Scientific, Inc.). Total proteins (50 μg) were then separated by 10% SDS-PAGE and electro-transferred onto nitrocellulose membranes. The membranes were blocked with phosphate-buffered saline (PBS) containing 5% non-fat milk overnight at 4˚C, incubated with the aforementioned primary antibodies overnight at 4˚C, and then with the aforementioned HRP-conjugated secondary antibodies for 2 h at room temperature. An enhanced chemiluminescence detection kit (Thermo Fisher Scientific, Inc.) was used for immunoblotting. Protein belts were exposed on the films in a dark room, then scanned and saved for the edition by Photoshop 7.0 software (Adobe Systems Inc., San Jose, CA, USA).

MTT assay. Cells ($5x10^3$ cells/well) were seeded in a 96-well plate and each sample was placed in 6 parallel wells. A total of 10 μl 5 mg/ml MTT (Beijing Solarbio Science & Technology Co., Ltd., Beijing, China) was added to each well for 4 h for

24, 48 or 72 h. The supernatant was then discarded, 100 μl DMSO was added and the plate was shaken with a Transference Decoloring Shaker (ZD-2008; Haimen Kylin-Bell Instrument Manufacturing Co., Ltd., Shanghai, China) at a fixed low speed at room temperature for 10 min. The optical density (OD) value was measured using a microplate reader (BioTek Instruments, Inc., Winooski, VT, USA) at a wavelength of 490 nm. The relative proliferative ratio of the cells per well was calculated according to the following formula: Relative proliferation (%) = ($OD_{transfection}/OD_{control}$) x 100%. The relative proliferative ratio of the blank control was set as 100% at all time points.

Colony formation analysis. Cells were seeded in media at a density of $2x10^3$ cells/well in 6-well plates (2 parallel wells/sample) for ~2 weeks at 37˚C in an incubator with an atmosphere containing 5% CO_2. When clear colonies were observed by the naked eye, the plates were washed three times with PBS and fixed with 100% methanol for 15 min at room temperature. The cells were then stained with crystal violet for 15 min at room temperature and washed with water to remove excess dye. Colonies containing >50 cells were counted under a light inverted microscope (Leica Microsystems GmbH, Wetzlar, Germany) at x100 magnification. Colony formation rate (%) = (means number of colonies/2000) x 100%. The experiment was repeated three times.

Wound healing assays. Cells were cultured overnight at 37˚C in an atmosphere containing 5% CO_2 to yield a monolayer in 6-well plates, and then the monolayer was scratched using 200-μl pipette tips, washed twice with PBS and RPMI-1640 medium was added. Wound healing status was monitored at 0, 12, 24 and 36 h, and images were captured with an inverted light microscope at x4 magnification in order to analyze the capability of cell migration in the 2-dimensional plane.

Transwell assays. The upper chambers of a Transwell plate with 8.0 μm pore size of polycarbonate membrane of polystyrene plates (cat. no. 3422; Costar, Corning Incorporated, Corning, NY, USA) were pretreated with heated serum-free RPMI-1640 medium for 30 min at 37˚C and then the medium was removed. Cells were adjusted to a concentration of $2x10^5$ cells/ml in RPMI-1640 medium with 0.2% FBS. A total of 200 μl sample was added to the upper chamber, and the lower chamber was filled 800 μl RPMI-1640 medium with 10% FBS. The plates were incubated at 37˚C for 24 h.

The upper chamber was removed, the medium was discarded and a cotton swab was used to remove cells on the bottom of the upper chamber. The remaining migrated cells on the back of the membrane in the bottom of upper chamber were fixed with 100% methanol for 10 min at room temperature and stained with 0.1% crystal violet for 10 min at room temperature for Transwell analysis in 3-dimensional space. Images were captured in 5 random visual fields under an inverted light microscope at x40 magnification. Experiments were repeated three times.

ELISA assays of autocrine IL-10 and IL-6. A total of $1x10^6$ cells/well were incubated in 24-well plates containing serum-free incomplete RPMI-1640 medium without the special indicator phenol red. After 24 h at 37˚C, the supernatant was collected for detection of autocrine IL-10 and IL-6 levels from the tumor cells using ELISA.

The absorbance value was measured at a wavelength of 450 nm with the Human IL-10 (cat. no. EK1102) and Human IL-6 (cat. no. EK1062) ELISA kits [Hangzhou Multi Sciences (Lianke) Biotech Co., Ltd., Hangzhou, China], according to the manufacturer's protocols.

Fluorescence-activated cell sorting (FACS) analysis. Cells were washed with ice-cold PBS and digested with 0.25% trypsin. Cells were collected for centrifugation at 697 x g for 5 min at room temperature, and the pellet was suspended with PBS as a single-cell solution, which was centrifuged at 697 x g at room temperature and washed twice with PBS. Cells were resuspended with 300 μl PBS and fixed with 700 μl 70% ethanol at 4˚C overnight for the detection of cell cycle distribution and apoptosis.

Cell cycle distribution and apoptosis were detected using FACS, which was performed by a specialized institute (Beijing Dingguo Changsheng Biotechnology Co., Ltd., Beijing, China).

Statistics. Statistical analysis was performed using the statistical software SPSS, version 17.0 (SPSS, Inc., Chicago, IL, USA). Data are presented as the mean ± standard deviation. Analysis of variance and least significant difference method were applied to perform multiple comparisons between the groups. $P<0.05$ was considered to indicate a statistically significant difference.

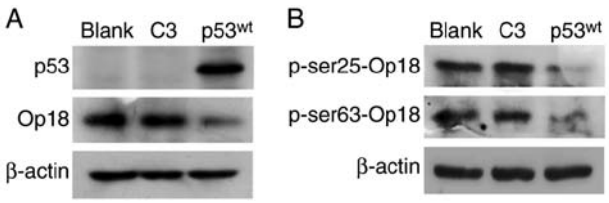

Figure 1. Introduction of exogenous *p53*^{wt} decreases Op18/stathmin expression and phosphorylation of NCI-H1299 cells. (A) Successfully expressed p53 downregulates the levels of Op18/stathmin in NCI-H1299 cells. (B) p53 inhibits Op18/stathmin phosphorylation at the Ser25 and Ser63 sites. Op18, oncoprotein 18; *p53*^{wt}, wild-type *p53*; C3, *pEGFP-C3*.

Results

Introduction of p53^{wt} *decreases Op18/stathmin expression and phosphorylation*. Western blotting for p53 demonstrated that the p53^{wt} lane exhibited a band while the blank and the C3 lanes did not exhibit any trace of p53, which demonstrated that the NCI-H1299 cells were originally p53-deficient, and that exogenous *p53*^{wt} was successfully introduced and expressed in the cells. There were no differences in the expression between the blank and the C3 controls, but the expression of Op18/stathmin was notably impaired in the p53^{wt} group, compared with the two control groups (Fig. 1A).

Similarly, the levels of Op18/stathmin phosphorylation at the Ser25 and Ser63 sites were notably decreased in the p53^{wt} group, compared with the two control groups, and there were no evident changes in the expression of Op18/stathmin at these two sites of phosphorylation between the blank and C3 control groups (Fig. 1B).

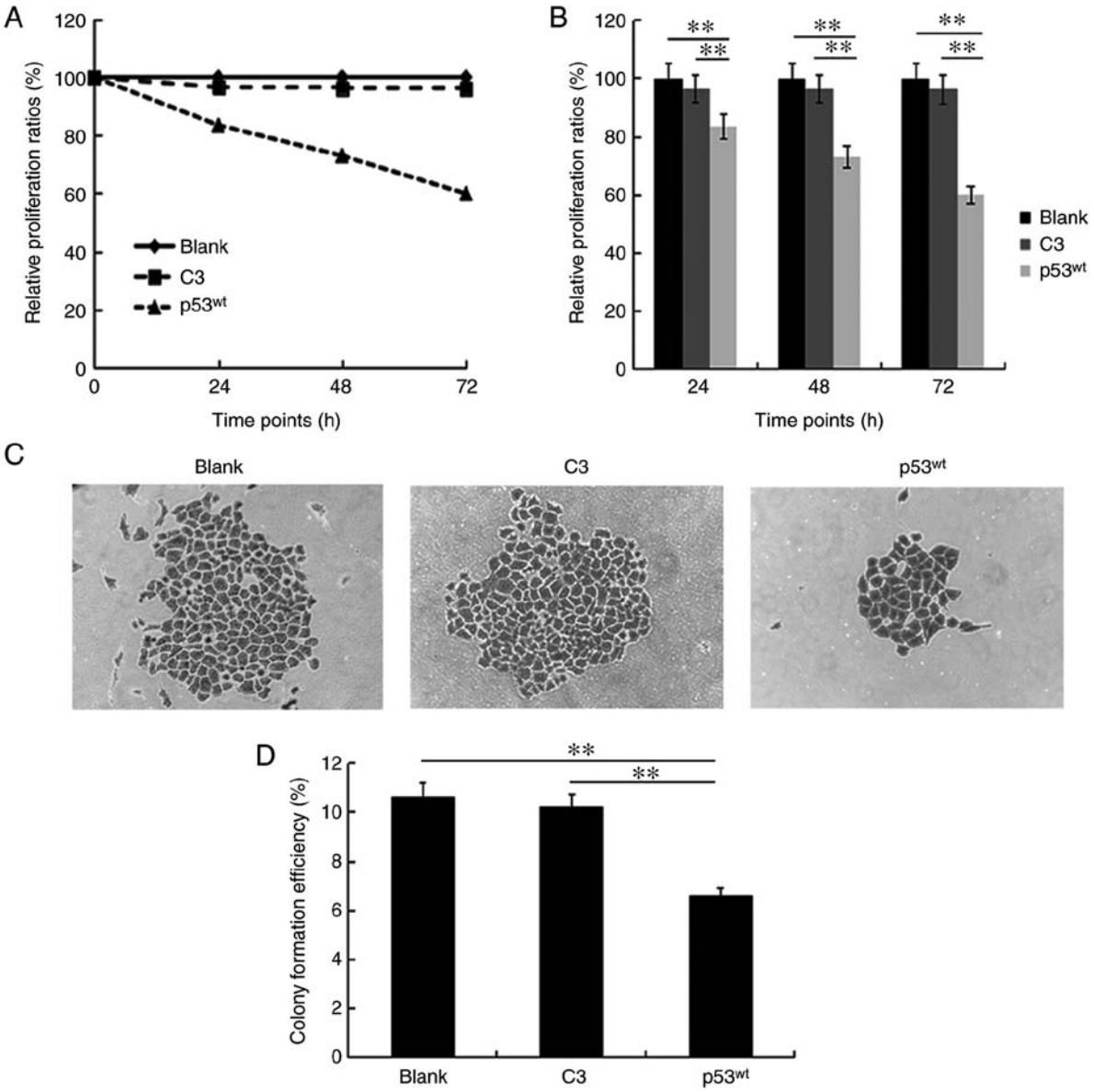

Figure 2. Exogenous *p53^{wt}* introduction attenuates the capacities of proliferation and colony formation in NCI-H1299 cells. (A) Cell proliferation curves of the three groups at different time points. (B) Histograms demonstrate that *p53^{wt}* introduction significantly inhibits cell proliferation, compared with the two control groups, at the three time points. (C) Images depict the status of colony formation in the three groups. (D) Histograms demonstrate the differences in the colony formation ratios of the three groups. Original magnification, x10. **P<0.01. *p53^{wt}*, wild-type *p53*; C3, *pEGFP-C3*.

p53 impairs the capabilities of cell proliferation and colony formation. Cell proliferation curves demonstrated that the relative proliferation ratios were 96.5, 96.3 and 96.2% in the C3 control group at the 24, 48 and 72 h time points, respectively, which were similar to the blank group, that was set as 100% at all time points. Compared with the two approximately parallel curves for the blank and C3 control groups, the representative curve for the p53^{wt} group descended steeply with proliferation ratios of 83.5, 72.9 and 59.9% at the three time points, respectively (Fig. 2A). The histograms demonstrated that no statistical difference existed between the blank and C3 control groups at the three time points, but the relative proliferation ratio of the p53^{wt} group was significantly reduced, compared with the two control groups at all time points (P<0.01; Fig. 2B).

Colony formation analysis demonstrated that a number of large colonies composed of several small colonies with merging borders, as depicted in the blank and C3 control groups. By contrast, there were only a few sparsely distributed small colonies in the p53^{wt} group (Fig. 2C). The mean colony formation ratios, which implied the mean percentage of forming colonies (>50 cells) in 2,000 cells, were 10.65 and 10.23% in the two control groups, respectively, and 6.62% in the p53^{wt} group, which was significantly reduced, compared with the other groups (P<0.01). The difference between the ratios of the two control groups was not significant (Fig. 2D).

p53 suppresses cell migration in multi-dimensional spaces. The wound healing assays demonstrated that a large proportion of the scratched area remained empty among all three groups at the 12 h time point. After 24 h, the wound width of the C3 group was reduced, compared with the blank group, but the difference was not notable by the naked eye. The wounds

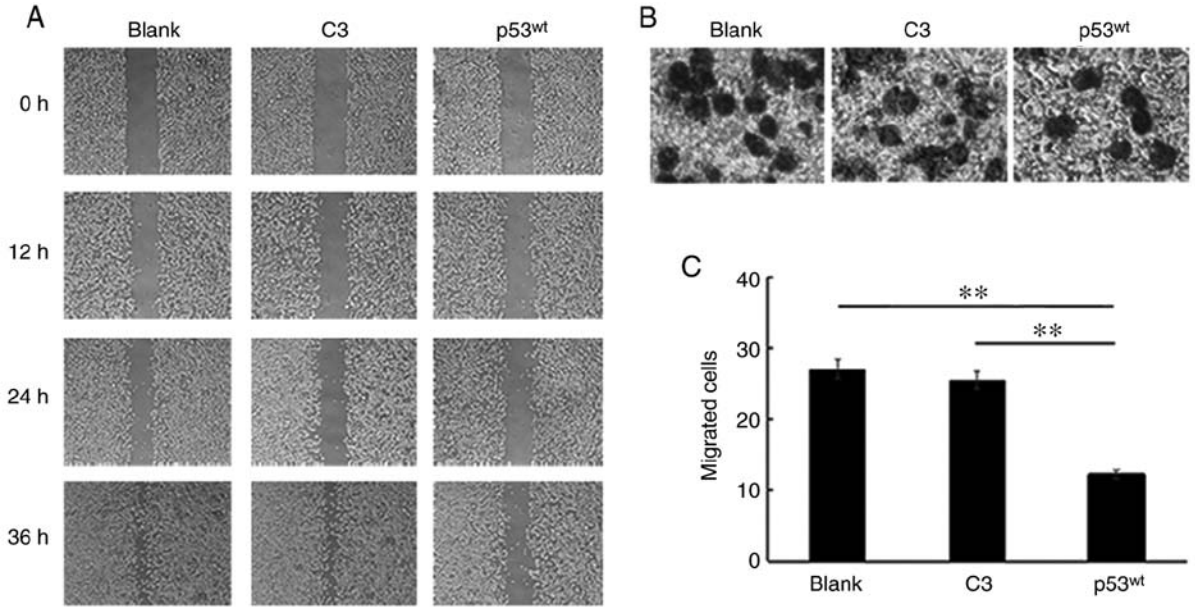

Figure 3. p53 inhibits migration of NCI-H1299 cells. (A) Images depict the status of cell migration in the 2-dimensional plane (original magnification, x4). (B) Transwell analysis demonstrates cell migration in the 3-dimensional space (original magnification, x40). (C) Histograms depict the differences in the number of migrated cells in the three groups. **P<0.01. *p53^{wt}*, wild-type *p53*; C3, *pEGFP-C3*.

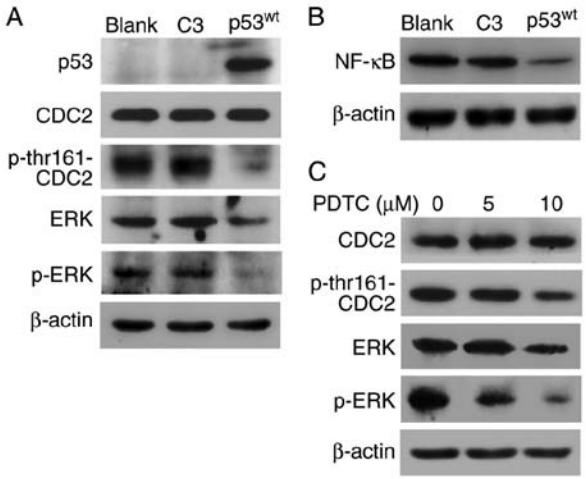

Figure 4. Western blot analysis of the effects of exogenous p53 on the activities of ERK and CDC2 kinases and transcription factor NF-κB in NCI-H1299 cells. (A) The expression and phosphorylation of ERK and CDC2 following p53 induction. (B) p53 inhibits the expression of NF-κB. (C) Concentration gradients of NF-κB inhibitor PDTC treatment. *p53^{wt}*, wild-type *p53*; C3, *pEGFP-C3*; CDC2, cyclin-dependent 2; ERK, extracellular signal-regulated kinase; NF-κB, nuclear factor-κB; PDTC, pyrrolidine dithiocarbamate; p, phospho.

had almost healed at 36 h in the blank and C3 control groups; however, a large area of the scratched region remained empty in the p53^{wt} group. *p53^{wt}* introduction inhibited the migration of NCI-H1299 cells in the 2-dimensional plane (Fig. 3A).

The Transwell assays identified that the mean number of migrated cells was 28, 26 and 14 among the blank, C3 and p53^{wt} groups, respectively. Therefore, the number of migrated cells was notably decreased following *p53^{wt}* introduction (Fig. 3B). Histograms indicated that there was no apparent difference in the number of infiltrating cells between the blank and C3 control groups, but the number of migrated cells was significantly reduced in the p53^{wt} group, compared with the two control groups; therefore, *p53^{wt}* significantly reduced the motility of cells in 3-dimensional space (P<0.01; Fig. 3C).

p53 negatively modulates the activities of CDC2 and ERK by inhibiting NF-κB expression. Western blotting indicated that p53 expression successfully attenuated CDC2 phosphorylation at the thr161 site. The levels of ERK and p-ERK were also downregulated in the p53^{wt} group, but those of CDC2 were similar among the three groups (Fig. 4A). Additionally, introduction of exogenous *p53^{wt}* reduced the expression of NF-κB (Fig. 4B).

The NF-κB inhibitor PDTC was employed to block NF-κB signaling in p53-deficient NCI-H1299 cells. Western blot analysis demonstrated that the levels of p-thr161-CDC2, ERK and p-ERK, with ERK being slightly decreased at 5 μM, compared with at 0 μM and notably reduced at 10 μM, while p-ERK gradually decreased in a PDTC concentration-dependent manner. Blockage of NF-κB signaling also downregulated the activities of p-thr161-CDC2 and ERK, which is in agreement with the results of p53 introduction, and the concentration gradient of PDTC did not exert any effects on CDC2 expression (Fig. 4C).

p53 inhibits IL-10 autocrine and protein expression. ELISA confirmed that the mean autocrine IL-10 OD level in the culture supernatant was 0.109, 0.093 and 0.055 in the blank, C3 and p53^{wt} groups, respectively. The mean level of the p53^{wt} group was significantly decreased, compared with the two control groups (P<0.01), and there was no significant difference between those of the blank and C3 control groups (Fig. 5A). ELISA demonstrated that IL-6 autocrine OD levels were low in the three groups and p53 did not affect IL-6 (Fig. 5B).

Western blot analysis demonstrated that IL-10 was expressed normally in the blank and C3 control groups, which

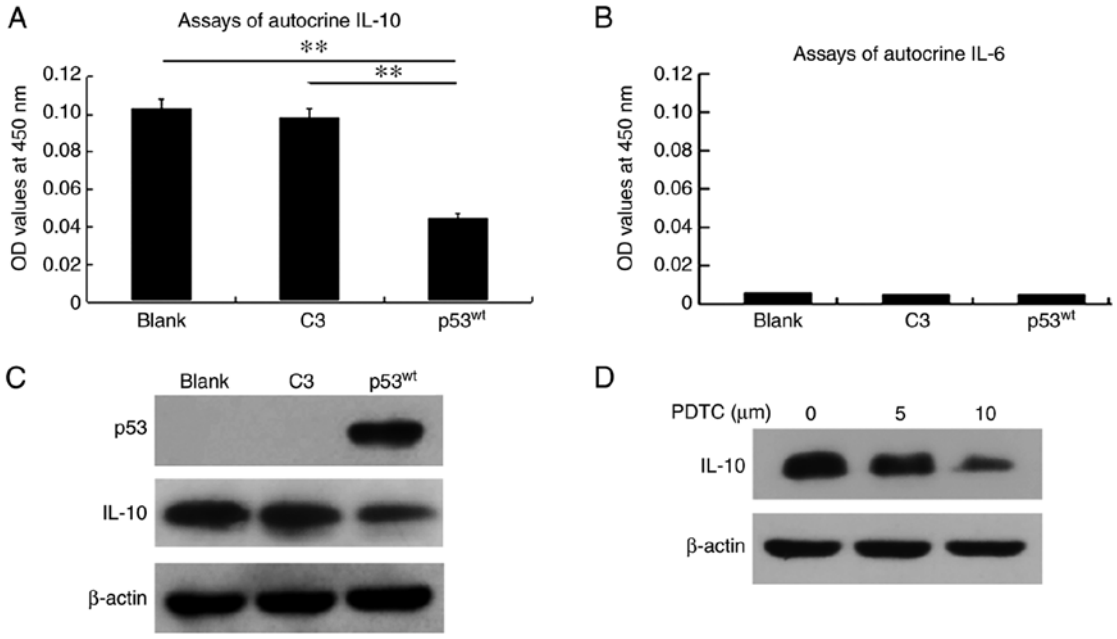

Figure 5. p53 inhibits autocrine IL-10 and IL-10 expression, but does not exert any effects on IL-6 in NCI-H1299 cells. (A) ELISA analysis demonstrates the difference in the levels of autocrine IL-10 among the three groups. (B) Autocrine IL-6 ELISA assays. (C) Western blot analysis depicts the expression of IL-10 following p53 induction. (D) Blocking of nuclear factor-κB with PDTC attenuated IL-10 expression in a concentration-dependent manner. **P<0.01. *p53*^{wt}, wild-type *p53*; *C3*, *pEGFP*-C3; IL, interleukin; PDTC, pyrrolidine dithiocarbamate.

was similar between them, but was notably attenuated in the p53^{wt} group. Additionally, IL-6 was not expressed in the three groups (Fig. 5C).

Concentration gradients of the inhibitor PDTC downregulated the expression of IL-10 in a concentration-dependent manner in NCI-H1299 cells, which implied that blockage of NF-κB signaling induced the identical inhibitory effects on IL-10 expression as exogenous *p53*^{wt} induction (Fig. 5D).

p53 induces cell cycle arrest at the G_1/S phases and cellular apoptosis. The images of cell growth demonstrated that cells were nearly confluent in the blank and C3 control groups, but there was reduced quantity of cells in the p53^{wt} group. FACS analysis validated that the proportion of cell that entered the G_2 phase was 25.94, 24.58 and 2.63% among the blank, C3 and p53^{wt} groups, respectively, while the cellular apoptosis ratios were 4.58, 5.82 and 9.24%, respectively. By contrast, the majority of NCI-H1299 cells were arrested at G_1/S phases when transfected with exogenous *p53*^{wt} (Fig. 6A).

The expression levels of caspase-3 and -9 were increased in the p53^{wt} group, compared with the two control groups, while no evident changes were observed in caspase-8 expression levels in the three groups (Fig. 6B). Introduction of p53 attenuated the expression of the anti-apoptotic protein Bcl-2, and upregulated the levels of its counterpart Bax (Fig. 6C). The expression levels of all of these molecules in the blank control group were similar to those in the C3 group (Fig. 6B and C).

p53 promotes the sensitivity of NCI-H1299 cells to Taxol. The images of cell growth demonstrated that there was a large amount of cells in the suspension in the three groups after 24 h treatment with 100 nM Taxol, and the adherent cells became significantly sparse in the p53^{wt} group, compared with the two control groups. FACS analysis indicated that the ratios of cell apoptosis were 11.23, 12.37 and 19.52% among the blank, C3 and p53^{wt} groups, respectively. The ratios of G_2 phase cells were 29.34, 28.59 and 15.79% among the blank, C3 and p53^{wt} groups, respectively. These results indicated that *p53*^{wt} introduction resulted in an increase in the cytotoxicity of Taxol in NCI-H1299 cells and a decrease in the ratios of cells at the G_2 phases (Fig. 7).

Discussion

p53 is a tumor suppressor gene that primarily arrests aberrant cells at the G_1/S phase checkpoint for repair of damaged DNA, which results in apoptosis when the degree of destroyed DNA is beyond the threshold of repair (5). Mutation of *p53* that occurs in the majority of tumors results in failure to control cell growth, apoptosis and DNA repair, and ultimately becomes a tumor-promoting gene that induces carcinogenesis and drug resistance (14). There are >50% of tumors that exhibit *p53* gene deficiency or mutation; therefore, utilization of *p53*^{wt} against tumors is an attractive treatment strategy (15,16).

Our previous studies confirmed that silencing Op18/stathmin would result in the inhibition of cell migration and invasion, which implied that the downregulation of Op18/stathmin expression was involved in the inhibition of cell migration and invasion in NCI-H1299 cells following the introduction of exogenous *p53*^{wt} (1,2). The present study confirmed that the introduction of exogenous *p53*^{wt} successfully inhibits Op18/stathmin expression and phosphorylation, and decreases the capacities of proliferation and colony formation, as well as migration in multi-dimensional spaces in NCI-H1299 cells. In melanoma A375, Hs294T and G361 cells, a previous study also determined that increased p53 expression

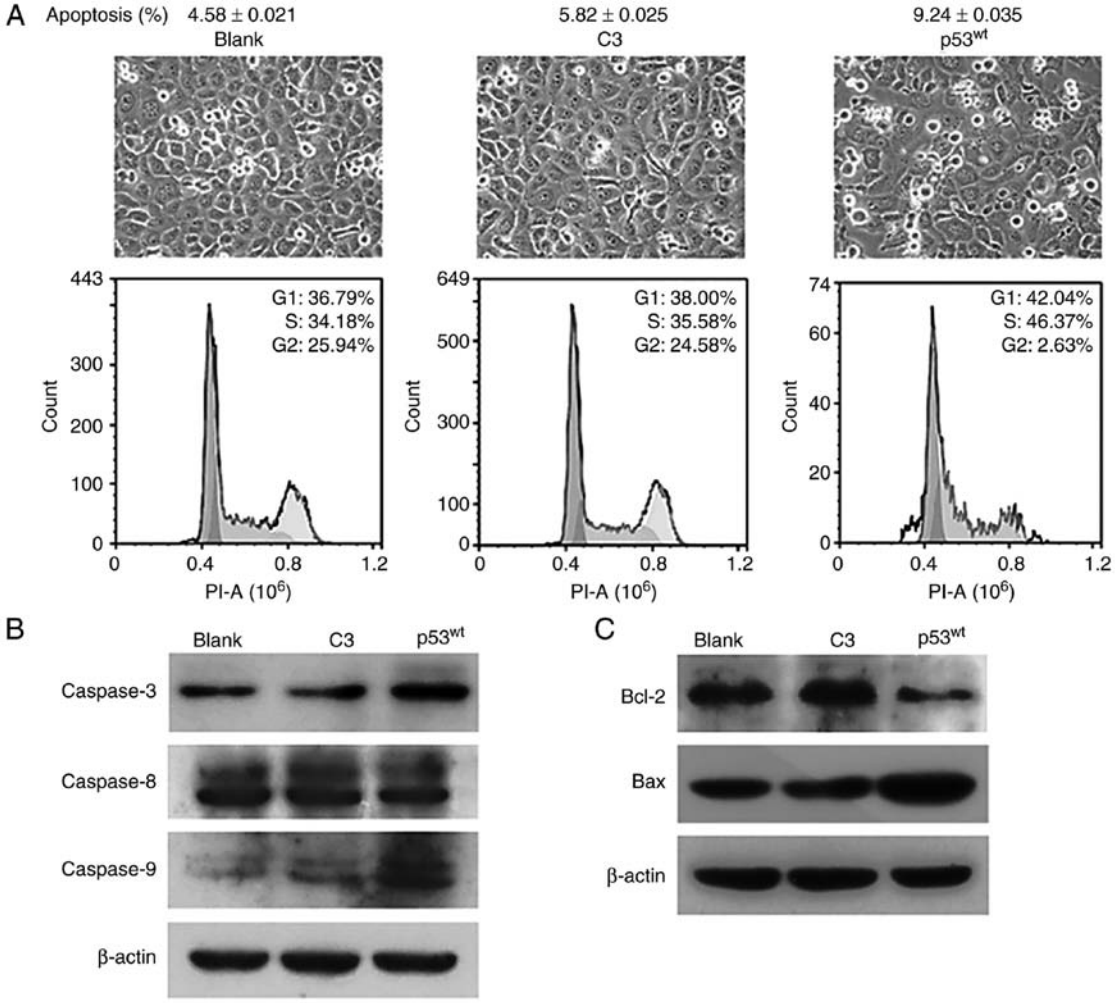

Figure 6. Analysis of growth and apoptosis in NCI-H1299 cells following p53 introduction. (A) The upper images depict the status of cell growth and the lower panels depict the cell cycle distribution and apoptosis ratios of the three groups as determined by fluorescence-activated cell sorting assays. (B) p53 initiates the activation of caspase-3 and -9. (C) p53 decreases Bcl-2 expression levels and increases Bax expression levels. Original magnification, x10. *p53*^{wt}, wild-type *p53*; C3, pEGFP-*C3*; Bcl-2, B-cell lymphoma 2; Bax, Bcl-2-associated X.

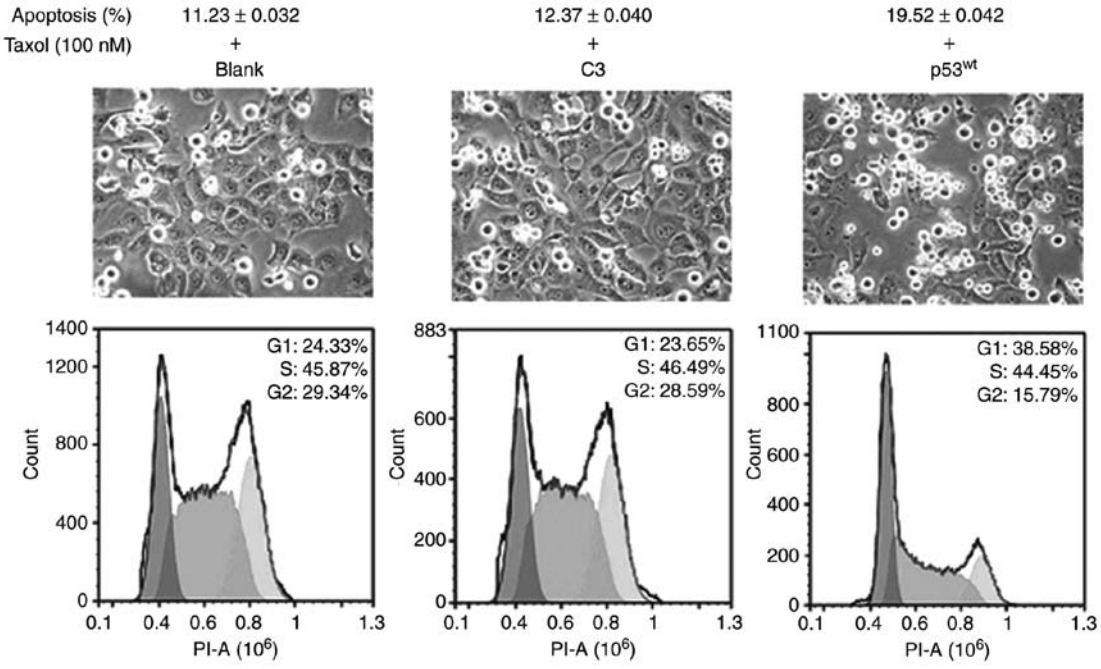

Figure 7. p53 induction promotes the sensitivity of NCI-H1299 cells to Taxol. The upper panel depicts the cell growth, and the lower panel depicts the FACS analysis of Taxol treatment. Original magnification, x10. *p53*^{wt}, wild-type *p53*; C3, *pEGFP-C3*.

resulted in inhibition of cellular growth and viability following treatment with the histone deacetylase sirtuin type 1 inhibitor Tenovin-1 (17).

The present study specifically demonstrated the status of Op18/stathmin expression and its phosphorylation following the introduction of exogenous $p53^{wt}$; however, further experiments primarily indicated the changes of regulatory molecules CDC2, ERK and NF-κB on Op18/stathmin signaling for the intervention of exogenous $p53^{wt}$ which negatively modulated the activities of CDC2 and ERK by inhibiting NF-κB expression. CDC2 is a positive regulator of the cell cycle process, in which aberrant activation is associated with acceleration of cell proliferation and malignant transformation in the development of tumors (18-20). ERK is a major member of the mitogen-activated protein kinases family, and is also involved in the positive regulation of cell proliferation and differentiation (21,22). In Epstein-Barr virus (EBV)-infected nasopharyngeal carcinoma CNE1 cells, Op18/stathmin was identified as the downstream target of CDC2 and ERK, and EBV-encoding latent membrane protein 1 promotes cell cycle progression through the regulation of CDC2- and ERK-mediated Op18/stathmin signaling (23,24). Previous studies indicated that Op18/stathmin was dephosphorylated in NCI-H1299 cells treated with the CDC2 blocker purvalanol A or ERK blocker PD98059, both of which enhance the sensitivity of cells to Taxol (25,26). Due to the activity of Op18/stathmin regulating microtubules being regulated by the balance of phosphorylation and dephosphorylation, the phosphorylation levels of Op18/stathmin at the Ser25 and 63 sites following the introduction of $p53^{wt}$ were detected. The present study demonstrated that exogenous $p53^{wt}$ expression inhibits the phosphorylation of CDC2-thr161 and ERK, downregulates the activities of CDC2 and ERK kinases, and negatively regulates Op18/stathmin phosphorylation at the Ser25 and Ser63 sites. The decreased phosphorylation of Op18/stathmin was associated with the downregulation of Op18/stathmin expression and the loss of the activities of its upstream kinases, ERK and CDC2, following exogenous $p53^{wt}$ introduction.

The transcription factor NF-κB is associated with cell proliferation, and blocking of NF-κB signaling results in inhibition of tumor growth (27,28). In the present study, introduction of exogenous $p53^{wt}$ decreased the expression levels of NF-κB and the activities of CDC2 and ERK, while PDTC blocking of NF-κB signaling also resulted in decreased levels of CDC2 and ERK activity in the NCI-H1299 cells. These results demonstrated that p53 negatively regulates the activation of CDC2 and ERK via NF-κB, and indirectly influences Op18/stathmin expression and phosphorylation. Therefore, p53 regulates Op18/stathmin signaling through the p53-NF-κB-CDC2/ERK-Op18/stathmin pathway.

IL-10 is a pleiotropic cytokine and is considered as an immunosuppressor that mediates tumor immune evasion through inhibition of the host immune response, therefore serving a vital role in tumor survival and metastasis (29). IL-6 is also a multi-functional cytokine secreted by a variety of cell types and is frequently involved in a series of physiological and pathological effects, including inflammation and fibrosis (30). Aberrant expression of IL-6 is associated with the poor prognosis of patients with glioma (31), and gallbladder and colon cancer types (32,33). The effects of $p53^{wt}$ on the release of autocrine cytokines IL-10 and IL-6 and their protein expression levels in NCI-H1299 cells were also investigated in the present study, which indicated that p53 inhibits IL-10 *in vitro* autocrine and protein expression, but does not exert any influence on IL-6. We hypothesized that p53-mediated Op18/stathmin signaling is implicated in the immune evasion of tumors via autocrine IL-10. However, IL-6 autocrine and expression remained at low levels in the NCI-H1299 cells with or without exogenous p53. A previous study reported that autocrine IL-10 suppressed the production of pro-inflammatory cytokines, including tumor necrosis factor-α, IL-1 and IL-6, and further mediated immune evasion by inhibiting the ability of antigen-presenting cells to present antigens to T cells (33).

Caspase-3 and -9 are the executor and promoter of the endogenous cell death pathway, respectively (25). Bcl-2 is an anti-apoptotic protein and Bax primarily acts against the anti-apoptotic activity of Bcl-2 (25,35,36). In the present study, p53 upregulated the expression levels of caspase-3 and -9, and Bax, and decreased the levels of Bcl-2 expression in NCI-H1299 cells. p53 resulted in cell cycle arrest at the G_1/S phases and an increase in cell apoptosis, enhancing the sensitivity of NCI-H1299 cells to Taxol, which indicates that the lack of p53 is associated with the development of Taxol resistance in NCI-H1299 cells with high expression of Op18/stathmin. Introduction of exogenous $p53^{wt}$ resulted in a majority of cells arresting at the G_1/S phases, but the ratios of NCI-H1299 cells halted at the G_1/S phases was only slightly reduced following the co-treatment of $p53^{wt}$ and Taxol, which may be associated with Taxol primarily inducing cells arresting at the G_2/M phase, eventually causing a decrease of G_1 stage cells following the synergistic induction of $p53^{wt}$ and Taxol, compared with the treatment of $p53^{wt}$ alone (37).

Acknowledgements

The authors would like to thank Professor Cao Ya from the Cancer Research Institute of Central South University (Changsha, China) for providing the plasmids.

Funding

This study was financed by the Key Scientific Research Project of Colleges and Universities of Hunan Province (grant no. 12A018), the National Natural Science Foundation of China (grant no. 81272274) and the Natural Science Foundation of Hunan Province (grant no. 12JJ3104).

Availability of data and materials

The datasets used and/or analyzed during the present study are available from the corresponding author on reasonable request.

Authors' contributions

XL was primarily responsible for the design of the study and the revision of the manuscript. The experiments, analysis and interpretation of the data were primarily conducted by SC. Members of the research team also included YZ, FS, DL and TY, who participated in part of the experiments, analysis and

interpretation of the data. All authors read and approved the final manuscript.

Ethics approval and consent to participate

Not applicable.

Patient consent for publication

Not applicable.

Competing interests

The authors declare that they have no competing interests.

References

1. Lin X, Liao Y, Yang J, Su L, Zou H and Zuo Y: Regulation of the drug-resistance of carcinoma cells mediated by Op18/stathmin. Chem Life 33: 265-268, 2013.
2. Long D, Yu T, Chen X, Liao Y and Lin X: RNAi targeting STMN alleviates the resistance to taxol and collectively contributes to down regulate the malignancy of NSCLC cells in vitro and in vivo. Cell Biol Toxicol 34: 7-21, 2018.
3. Guntur VP, Waldrep JC, Guo JJ, Selting K and Dhand R: Increasing p53 protein sensitizes non-small cell lung cancer to paclitaxel and cisplatin in vitro. Anticancer Res 30: 3557-3564, 2010.
4. Lv Y, Huo Y, Yu X, Liu R, Zhang S, Zheng X and Zhang X: TopBP1 contributes to the chemoresistance in non-small cell lung cancer through upregulation of p53. Drug Des Devel Ther 10: 3053-3064, 2016.
5. Riley T, Sontag E, Chen P and Levine A: Transcriptional control of human p53-regulated genes. Nat Rev Mol Cell Biol 9: 402-412, 2008.
6. Matt S and Hofmann TG: The DNA damage-induced cell death response: A roadmap to kill cancer cells. Cell Mol Life Sci 73: 2829-2850, 2016.
7. Zhang EB, Yin DD, Sun M, Kong R, Liu XH, You LH, Han L, Xia R, Wang KM, Yang JS, *et al*: P53-regulated long non-coding RNA TUG1 affects cell proliferation in human non-small cell lung cancer, partly through epigenetically regulating HOXB7 expression. Cell Death Dis 5: e1243, 2014.
8. Kracikova M, Akiri G, George A, Sachidanandam R and Aaronson SA: A threshold mechanism mediates p53 cell fate decision between growth arrest and apoptosis. Cell Death Differ 20: 576-588, 2013.
9. Lin X and Cao Y: Advances in the regulation of the signals on Op18/stathmin. Life Sci Res 11: 195-199, 2007.
10. Cassimeris L: The oncoprotein 18/stathmin family of microtubule destabilizers. Curr Opin Cell Biol 14: 18-24, 2002.
11. Belletti B and Baldassarre G: Stathmin: A protein with many tasks. New biomarker and potential target in cancer. Expert Opin Ther Targets 15: 1249-1266, 2011.
12. Johnsen JI, Aurelio ON, Kwaja Z, Jörgensen GE, Pellegata NS, Plattner R, Stanbridge EJ and Cajot JF: p53-mediated negative regulation of stathmin/Op18 expression is associated with G_2/M cell-cycle arrest. Int J Cancer 88: 685-691, 2000.
13. Bessho R, Matsubara K, Kubota M, Kuwakado K, Hirota H, Wakazono Y, Lin YW, Okuda A, Kawai M and Nishikomori R: Pyrrolidine dithiocarbamate, a potent inhibitor of nuclear factor kappa B (NF-kappa B) activation, prevents apoptosis in human promyelocytic leukemia HL-60 cells and thymocytes. Biochem Pharmacol 48: 1883-1889, 1994.
14. Shen F, Wu Y and Lin X: The pleiotropic function of P53. Basic Clin Med 35: 1672-1676, 2015 (In Chinese).
15. Olive KP, Tuveson DA, Ruhe ZC, Yin B, Willis NA, Bronson RT, Crowley D and Jacks T: Mutant p53 gain of function in two mouse models of Li-Fraumeni syndrome. Cell 119: 847-860, 2004.
16. Fuster JJ, Sanz-Gonzalez SM, Moll UM and Andres V: Classic and novel roles of p53: Prospects for anticancer therapy. Trends Mol Med 13: 192-199, 2007.
17. Wilking MJ, Singh C, Nihal M, Zhong W and Ahmad N: SIRT1 deacetylase is overexpressed in human melanoma and its small molecule inhibition imparts anti-proliferative response via p53 activation. Arch Biochem Biophys 563: 94-100, 2014.
18. Liu P, Kao TP and Huang H: CDK1 promotes cell proliferation and survival via phosphorylation and inhibition of FOXO1 transcription factor. Oncogene 27: 4733-4744, 2008.
19. Malumbres M and Barbacid M: Cell cycle, CDKs and cancer: A changing paradigm. Nat Rev Cancer 9: 153-166, 2009.
20. Perez de Castro I, de Carcer G and Malumbres M: A census of mitotic cancer genes: New insights into tumor cell biology and cancer therapy. Carcinogenesis 28: 899-912, 2007.
21. Dhillon AS, Hagan S, Rath O and Kolch W: MAP kinase signalling pathways in cancer. Oncogene 26: 3279-3290, 2007.
22. Wang J and Wu GS: Role of autophagy in cisplatin resistance in ovarian cancer cells. J Biol Chem 289: 17163-17173, 2014.
23. Lin X, Liu S, Luo X, Ma X, Guo L, Li L, Li Z, Tao Y and Cao Y: EBV-encoded LMP1 regulates Op18/stathmin signaling pathway by cdc2 mediation in nasopharyngeal carcinoma cells. Int J Cancer 124: 1020-1027, 2009.
24. Lin X, Tang M, Tao Y, Li L, Liu S, Guo L, Li Z, Ma X, Xu J and Cao Y: Epstein-Barr virus-encoded LMP1 triggers regulation of the ERK-mediated Op18/stathmin signaling pathway in association with cell cycle. Cancer Sci 103: 993-999, 2012.
25. Chen X, Liao Y, Long D, Yu T, Shen F and Lin X: The Cdc2/Cdk1 inhibitor, purvalanol A, enhances the cytotoxic effects of taxol through Op18/stathmin in non-small cell lung cancer cells *in vitro*. Int J Mol Med 40: 235-242, 2017.
26. Lin X, Liao Y, Chen X, Long D, Yu T and Shen F: Regulation of oncoprotein 18/stathmin signaling by ERK concerns the resistance to taxol in nonsmall cell lung cancer cells. Cancer Biother Radiopharm 31: 37-43, 2016.
27. Huan L, Bao C, Chen D, Li Y, Lian J, Ding J, Huang S, Liang L and He X: MicroRNA-127-5p targets the biliverdin reductase B/nuclear factor-κB pathway to suppress cell growth in hepatocellular carcinoma cells. Cancer Sci 107: 258-266, 2016.
28. Lu Y, Liu C, Cheng H, Xu Y, Jiang J, Xu J, Long J, Liu L and Yu X: Stathmin, interacting with Nf-κB, promotes tumor growth and predicts poor prognosis of pancreatic cancer. Curr Mol Med 14: 328-339, 2014.
29. Incrocci R, Barse L, Stone A, Vagvala S, Montesano M, Subramaniam V and Swanson-Mungerson M: Epstein-barr virus latent membrane protein 2A (LMP2A) enhances IL-10 production through the activation of Bruton's tyrosine kinase and STAT3. Virology 500: 96-112, 2017.
30. Kawaratani H, Moriya K, Namisaki T, Uejima M, Kitade M, Takeda K, Okura Y, Kaji K, Takaya H, Nishimura N, *et al*: Therapeutic strategies for alcoholic liver disease: Focusing on inflammation and fibrosis (Review). Int J Mol Med 40: 263-270, 2017.
31. Shan Y, He X, Song W, Han D, Niu J and Wang J: Role of IL-6 in the invasiveness and prognosis of glioma. Int J Clin Exp Med 8: 9114-9120, 2015.
32. Zhang M, Gong W, Zhang Y, Yang Y, Zhou D, Weng M, Qin Y, Jiang A, Ma F and Quan Z: Expression of interleukin-6 is associated with epithelial-mesenchymal transition and survival rates in gallbladder cancer. Mol Med Rep 11: 3539-3546, 2015.
33. Olsen J, Kirkeby LT, Olsen J, Eiholm S, Jess P, Gögenur I and Troelsen JT: High interleukin-6 mRNA expression is a predictor of relapse in colon cancer. Anticancer Res 35: 2235-2240, 2015.
34. Mittal SK and Roche PA: Suppression of antigen presentation by IL-10. Curr Opin Immunol 34: 22-27, 2015.
35. Klumpp D, Misovic M, Szteyn K, Shumilina E, Rudner J and Huber SM: Targeting TRPM2 channels impairs radiation-induced cell cycle arrest and fosters cell death of T cell leukemia cells in a Bcl-2-dependent manner. Oxid Med Cell Longev 2016: 8026702, 2016.
36. Veena VK, Kennedy K, Lakshmi P, Krishna R and Sakthivel N: Anti-leukemic, anti-lung, and anti-breast cancer potential of the microbial polyketide 2,4-diacetylphloroglucinol (DAPG) and its interaction with the metastatic proteins than the antiapoptotic Bcl-2 proteins. Mol Cell Biochem 414: 47-56, 2016.
37. Oyaizu H, Adachi Y, Okumura T, Okigaki M, Oyaizu N, Taketani S, Ikebukuro K, Fukuhara S and Ikehara S: Proteasome inhibitor 1 enhances paclitaxel-induced apoptosis in human lung adenocarcinoma cell line. Oncol Rep 8: 825-829, 2001.